

# Chapter 39

## NEUTRINOS

Photons carry  $\hbar$  of angular momentum in their electric and magnetic fields as shown in the Photon section. All electronic transitions require  $\hbar$  of angular momentum photons. Nuclear reactions such as beta decay require emission of neutrinos with  $\frac{\hbar}{2}$  of angular momentum. Thus, they may be photons with different electric and magnetic fields that give  $\frac{\hbar}{2}$  of angular momentum. Then different trigonometric functions of the electric and magnetic fields would correspond to the different flavor neutrinos, the energy of each would depend on its frequency since the speed is light speed, and the cross sections would depend on the particular fields and energy.

To conserve energy and linear and angular momentum an electron antineutrino,  $\bar{\nu}_e$ , is emitted with the beta particle. The antineutrino is a **unique elliptically polarized photon** that has handedness (the neutrino and antineutrino have opposite handedness), is massless, and travels at the speed  $c$ . Consider the photon atomic orbital given in the Equation of the Photon section. It may comprise magnetic and electric field lines basis elements that are constant in magnitude as a function of angle over the surface. Or, the magnitude may vary as a function of angular position  $(\phi, \theta)$  on the atomic orbital which corresponds to an elliptically polarized photon. The general photon equation for the electric field is

$$\mathbf{E}_{\phi, \theta} = \frac{e}{4\pi\epsilon_0 r_{\text{photon}}^2} \left( -1 + \frac{1}{n} \left[ Y_0^0(\theta, \phi) + \text{Re} \left\{ Y_\ell^m(\theta, \phi) e^{i\omega_n t} \right\} \right] \right) \delta \left( r - \frac{\lambda}{2\pi} \right) \quad (39.12)$$

For the particle-production or emission event,  $r_{\text{photon}}$  is the radius of the photon atomic orbital which is equal to  $\pi \Delta n a_H$ , the change in electron atomic orbital radius given by Eq. (2.21),  $\lambda$  is the photon wavelength which is equal to  $\Delta \lambda$ , the change in the de Broglie wavelength of the atomic orbital given by Eqs. (2.21), (1.34), and (1.38), and  $\omega_n = \frac{2\pi c}{\lambda}$  is the photon angular velocity which is equal to  $\Delta \omega$ , the change in atomic orbital angular velocity given by Eqs. (2.21). The magnetic field photon atomic orbital is given by Eqs. (4.14) and (4.2). The nature of the unique elliptically polarized photon atomic orbital which is the antineutrino (neutrino) is determined by the nature of quark/gluon functions and the change in the quark/gluon angular harmonic functions during the transition from a neutron to a proton (proton to a neutron) with the emission of a beta particle (positron). A free quark or a free gluon is not a stable state of matter, and both are precluded from existence in isolation. Quarks and gluons can only exist in pairs, each comprising a quark and a gluon. In the case of beta decay, a down quark/gluon is converted to an up quark/gluon. Energy and linear momentum are conserved by the emission of an electron antineutrino,  $\bar{\nu}_e$ , with the beta particle where the maximum energy of the antineutrino is that of the mass deficit. To conserve angular momentum, the electric field,  $\mathbf{E}_\theta$ , of the electron antineutrino has an angular dependence given by a harmonic function squared corresponding to the change between the initial and final quark/gluon functions where the electric field of each gluon and its corresponding quark are radial and Eq. (37.34) applies.

$$\mathbf{E}_\theta \propto \text{Re} \left\{ \left( Y_\ell^m(\theta, \phi) \right)^2 \left( 1 + e^{i\omega_n t} \right) \right\} \delta \left( r - \frac{\lambda}{2\pi} \right) \quad (39.13)$$

$$\propto \cos^2 \theta \text{Re} \left( 1 + e^{i\omega_n t} \right) \delta \left( r - \frac{\lambda}{2\pi} \right) = \left( \frac{1}{2} + \frac{\cos 2\theta}{2} \right) \text{Re} \left( 1 + e^{i\omega_n t} \right) \delta \left( r - \frac{\lambda}{2\pi} \right)$$

where  $\ell=1$  and the power is given by Eq. (4.16). In contrast, the electric field of a photon corresponding to electronic transitions (Eq. (39.12)) is given by the sum of a constant function plus a spherical harmonic modulation function which averages to zero over a period. The angular momentum of an antineutrino (neutrino) is  $-\frac{\hbar}{2}$  ( $\frac{\hbar}{2}$ )

$$|\mathbf{m}| = \int \frac{1}{8\pi c} \text{Re} [\mathbf{r} \times (\mathbf{E} \times \mathbf{B}^*)] dx^4 = \frac{\hbar}{2} \quad (39.14)$$

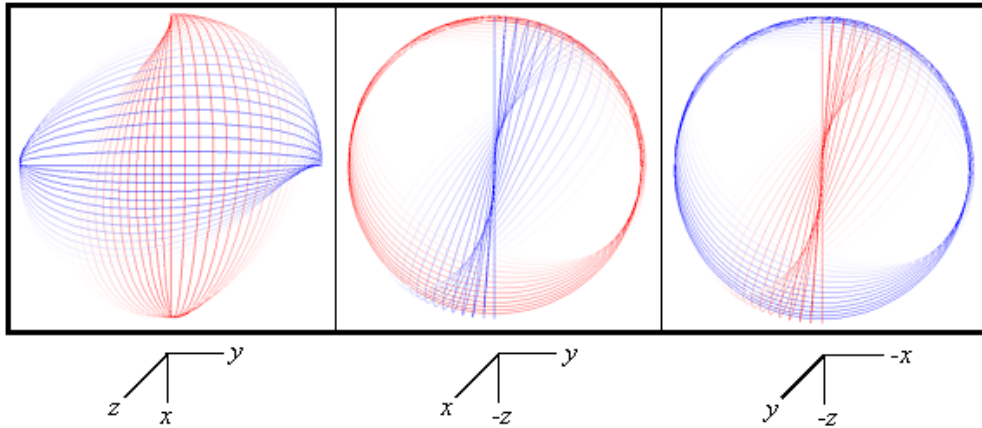
compared to that of a photon corresponding to an electronic transition of  $\pm \hbar$  (Eq. (4.1)).

The matrices to generate the electric and magnetic vector fields (e&mvf) of neutrinos are the same as those of the right- and left-circularly-polarized and linearly-polarized photons with the exception that the magnitude of the basis element field is not constant over the spherical surface, but is modulated by a trigonometric function squared. The right- and left- $\cos^2 \theta$  or  $\sin^2 \theta$ -polarized neutrinos are mirror images of opposite spin corresponding to a neutrino-antineutrino pair. The right-hand- $\cos^2 \theta$ -polarized neutrino ( $RHC^2P$ ) is given by:

$$\begin{bmatrix} x' \\ y' \\ z' \end{bmatrix} = \cos^2 \theta \delta(r - r_{\text{photon}}) \begin{bmatrix} \frac{1}{2} + \frac{\cos \theta}{2} & \frac{1}{2} - \frac{\cos \theta}{2} & -\frac{\sin \theta}{\sqrt{2}} \\ \frac{1}{2} - \frac{\cos \theta}{2} & \frac{1}{2} + \frac{\cos \theta}{2} & \frac{\sin \theta}{\sqrt{2}} \\ \frac{\sin \theta}{\sqrt{2}} & -\frac{\sin \theta}{\sqrt{2}} & \cos \theta \end{bmatrix} \cdot \left( E_0 \begin{bmatrix} 0 \\ r_n \cos \phi \\ r_n \sin \phi \end{bmatrix}_{\text{Red}} + B_0 \begin{bmatrix} r_n \cos \phi \\ 0 \\ r_n \sin \phi \end{bmatrix}_{\text{Blue}} \right) \quad (39.15)$$

The  $RHC^2P$  neutrino-e&mvf that is generated by the rotation of the great-circle basis elements in the  $xz$ - and  $yz$ -planes about the  $(\mathbf{i}_x, \mathbf{i}_y, 0\mathbf{i}_z)$ -axis by  $\frac{\pi}{2}$  corresponding to the output of the matrix given by Eq. (39.15) is shown in Figure 39.1 wherein the magnitude of each field line is according to  $\cos^2 \theta$ .

**Figure 39.1.** The field-line pattern given by Eq. (39.15) from three orthogonal perspectives of a  $RHC^2P$  neutrino-e&mvf corresponding to the first great circle magnetic field line and the second great circle electric field line shown with 6 degree increments of the angle  $\theta$ . (Electric field lines red; Magnetic field lines blue).

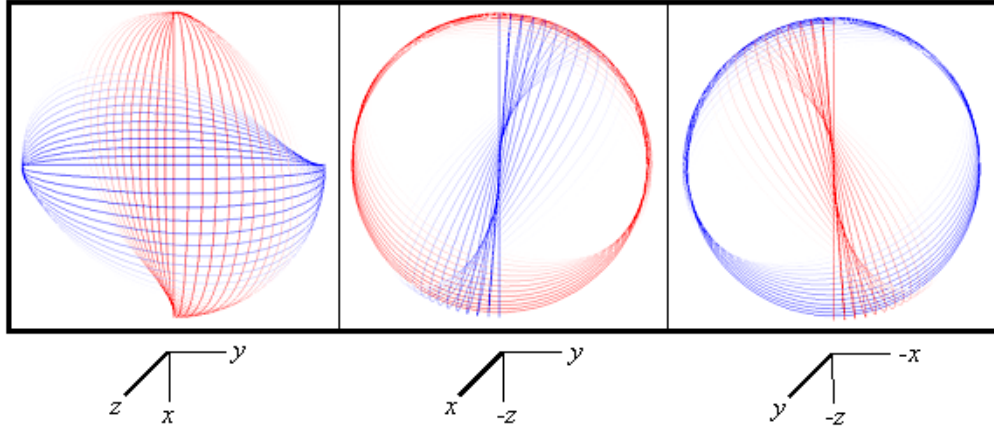


The corresponding antineutrino, the left-hand- $\cos^2 \theta$ -polarized neutrino ( $LHC^2P$ ), is given by:

$$\begin{bmatrix} x' \\ y' \\ z' \end{bmatrix} = \cos^2 \theta \delta(r - r_{\text{photon}}) \begin{bmatrix} \frac{1}{2} + \frac{\cos \theta}{2} & -\frac{1}{2} + \frac{\cos \theta}{2} & \frac{\sin \theta}{\sqrt{2}} \\ -\frac{1}{2} + \frac{\cos \theta}{2} & \frac{1}{2} + \frac{\cos \theta}{2} & \frac{\sin \theta}{\sqrt{2}} \\ \frac{\sin \theta}{\sqrt{2}} & -\frac{\sin \theta}{\sqrt{2}} & \cos \theta \end{bmatrix} \cdot \left( E_0 \begin{bmatrix} 0 \\ r_n \cos \phi \\ r_n \sin \phi \end{bmatrix}_{\text{Red}} + B_0 \begin{bmatrix} r_n \cos \phi \\ 0 \\ r_n \sin \phi \end{bmatrix}_{\text{Blue}} \right) \quad (39.16)$$

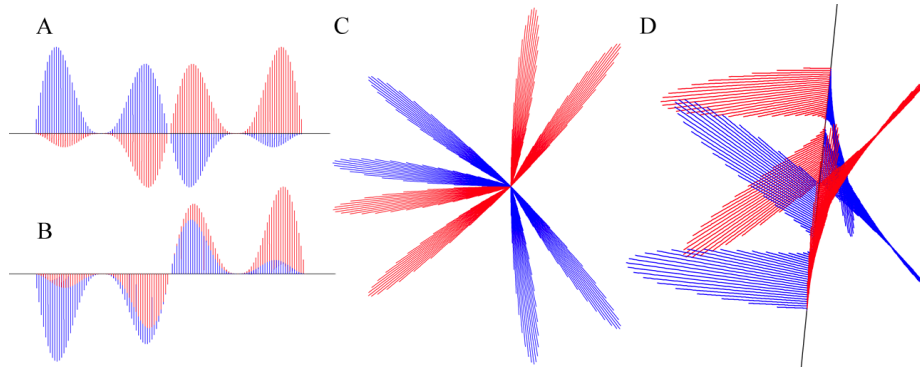
The  $LHC^2P$  neutrino-e&mvf that is generated by the rotation of the great-circle basis elements in the  $xz$ - and  $yz$ -planes about the  $(\mathbf{i}_x, -\mathbf{i}_y, 0\mathbf{i}_z)$ -axis by  $\frac{\pi}{2}$  corresponding to the output of the matrix given by Eq. (39.16) is shown in Figure 39.2.

**Figure 39.2.** The field-line pattern given by Eq. (39.16) from three orthogonal perspectives of a  $LHC^2P$  neutrino-e&mvf corresponding to the first great circle magnetic field line and the second great circle electric field line shown with 6 degree increments of the angle  $\theta$ . (Electric field lines red; Magnetic field lines blue).



Based on the invariance of the field lines under Gauss' Integral Law as given in the Photon section, the spatial distribution of the field lines of a cosine-squared neutrino (Eq. (39.13)) in the inertial frame for the stationary observer or laboratory frame is shown in Figure 39.3.

**Figure 39.3.** The electric (red) and magnetic (blue) field lines of a cosine-squared neutrino given by Eq. (39.13) as seen along the axis of propagation in the lab inertial reference frame at a fixed time. A and B. Views transverse to the axis of propagation, the z-axis, wherein  $2r_{neutrino} = \lambda$ . C and D. Off z-axis views showing field aspects both along and transverse to the axis of propagation.



Eq. (39.13) is the equation of the neutrino's electric field in its frame. The neutrino's field called the neutrino electric and magnetic vector field (neutrino-e&mvf) follows from that of the photon. Eq. (25) of Appendix V: Analytical-Equation Derivation of the Photon Electric and Magnetic Fields which gives the laboratory-frame relationship of the fields and the angular momentum then becomes:

$$\frac{1}{8\pi c} \sqrt{\frac{\epsilon_0}{\mu_0}} \frac{E_0^2}{4} \frac{2\pi}{2\omega} 2\pi r_{photon}^3 \int_0^\pi \sin^2 2\theta \cos^2 \theta \sin^4 \theta d\theta = \frac{\hbar}{2} \quad (39.17)$$

$$\sqrt{\frac{\epsilon_0}{\mu_0}} \frac{E_0^2}{32c} \frac{2\pi}{\omega} r_{photon}^3 \int_0^\pi \sin^2 2\theta \left( \frac{1 + \cos 2\theta}{2} \right) \left( \frac{1 - \cos 2\theta}{2} \right)^2 d\theta = \frac{\hbar}{2} \quad (39.18)$$

$$\sqrt{\frac{\epsilon_0}{\mu_0}} \frac{E_0^2}{256c} \frac{2\pi}{\omega} r_{photon}^3 \int_0^\pi \sin^2 2\theta (1 - \cos 2\theta - \cos^2 2\theta + \cos^3 2\theta) d\theta = \frac{\hbar}{2} \quad (39.19)$$

Using the wave equation relationship and the relationship between the wavelength and the radius of the photon-e&mvf given by Eq. (21) and Eq. (22) of Appendix V, respectively, gives

$$\sqrt{\frac{\epsilon_0}{\mu_0}} \frac{E_0^2 \pi^4}{128 \omega^4} c^2 \left( \begin{array}{c} \int_0^\pi \sin^2 2\theta d\theta - \int_0^\pi \sin^2 2\theta \cos 2\theta d\theta \\ - \int_0^\pi \sin^2 2\theta \cos^2 2\theta d\theta + \int_0^\pi \sin^2 2\theta \cos^3 2\theta d\theta \end{array} \right) = \frac{\hbar}{2} \quad (39.20)$$

The integrals by Lide [2] give

$$\sqrt{\frac{\epsilon_0}{\mu_0}} \frac{E_0^2 \pi^4}{128 \omega^4} c^2 \left( \begin{array}{c} \left( \frac{\theta}{2} - \frac{1}{8} \sin 4\theta \right)_0^\pi - \left( \frac{\sin^3 2\theta}{6} \right)_0^\pi \\ - \left( -64 \sin 8\theta + \frac{\theta}{8} \right)_0^\pi + \left( -\frac{\sin 2\theta \cos^4 2\theta}{10} \right)_0^\pi \\ + \frac{1}{5} \int_0^\pi \cos^3 2\theta d\theta \end{array} \right) = \frac{\hbar}{2} \quad (39.21)$$

$$\sqrt{\frac{\epsilon_0}{\mu_0}} \frac{E_0^2 \pi^4}{128 \omega^4 \sqrt{\epsilon_0 \mu_0}} c \left( \frac{\pi}{2} - \frac{\pi}{8} + \frac{1}{30} \left( \sin 2\theta (\cos^2 2\theta + 2) \right)_0^\pi \right) = \frac{\hbar}{2} \quad (39.22)$$

$$\sqrt{\frac{\epsilon_0}{\mu_0}} \frac{E_0^2 \pi^4}{128 \omega^4 \sqrt{\epsilon_0 \mu_0}} c \left( \frac{\pi}{2} - \frac{\pi}{8} \right) = \frac{\hbar}{2} \quad (39.23)$$

$$\frac{3E_0^2}{1024} \frac{\pi^5}{\omega^4 \mu_0} c = \frac{\hbar}{2} \quad (39.24)$$

Thus,

$$E_0 = \sqrt{\frac{512 \omega^4 \mu_0 \hbar}{3c\pi^5}} = \omega^2 \sqrt{\frac{512 \mu_0 \hbar}{3c\pi^5}} \quad (39.25)$$

which has the required MKS units of  $Vm^{-1}$ . From Planck's law, the energy is given by:

$$E = L\omega = \frac{\hbar}{2} \omega = \frac{3E_0^2}{1024} \frac{\pi^5}{\omega^4 \mu_0} c\omega \quad (39.26)$$

In the case of Eq. (39.13), a neutrino of a different flavor can also have an electric field in its frame of:

$$\mathbf{E}_\theta \propto \text{Re} \left\{ \left( Y_\ell^m(\theta, \phi) \right)^2 \left( 1 + e^{i\omega_n t} \right) \right\} \delta \left( r - \frac{\lambda}{2\pi} \right) \quad (39.27)$$

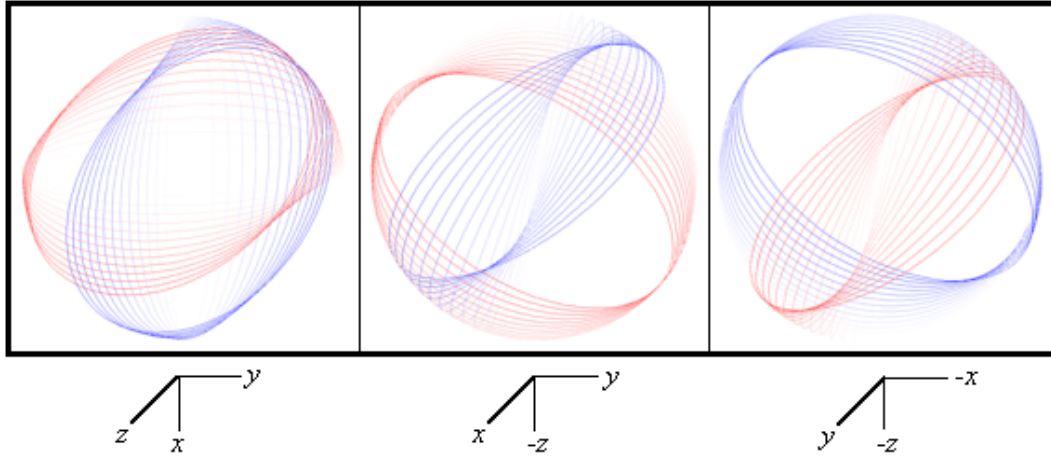
$$\propto \sin^2 \theta \text{Re} \left( 1 + e^{i\omega_n t} \right) \delta \left( r - \frac{\lambda}{2\pi} \right) = \left( \frac{1}{2} - \frac{\cos 2\theta}{2} \right) \text{Re} \left( 1 + e^{i\omega_n t} \right) \delta \left( r - \frac{\lambda}{2\pi} \right)$$

The right-hand- $\sin^2 \theta$ -polarized neutrino ( $RHS^2P$ ) is given by:

$$\begin{bmatrix} x' \\ y' \\ z' \end{bmatrix} = \sin^2 \theta \delta(r - r_{\text{photon}}) \begin{bmatrix} \frac{1}{2} + \frac{\cos \theta}{2} & \frac{1}{2} - \frac{\cos \theta}{2} & -\frac{\sin \theta}{\sqrt{2}} \\ \frac{1}{2} - \frac{\cos \theta}{2} & \frac{1}{2} + \frac{\cos \theta}{2} & \frac{\sin \theta}{\sqrt{2}} \\ \frac{\sin \theta}{\sqrt{2}} & -\frac{\sin \theta}{\sqrt{2}} & \cos \theta \end{bmatrix} \cdot \left( E_0 \begin{bmatrix} 0 \\ r_n \cos \phi \\ r_n \sin \phi \end{bmatrix}_{\text{Red}} + B_0 \begin{bmatrix} r_n \cos \phi \\ 0 \\ r_n \sin \phi \end{bmatrix}_{\text{Blue}} \right) \quad (39.28)$$

The  $RHS^2P$  neutrino-e&mvf that is generated by the rotation of the great-circle basis elements in the  $xz$ - and  $yz$ -planes about the  $(\mathbf{i}_x, \mathbf{i}_y, 0\mathbf{i}_z)$ -axis by  $\frac{\pi}{2}$  corresponding to the output of the matrix given by Eq. (39.28) is shown in Figure 39.4.

**Figure 39.4.** The field-line pattern given by Eq. (39.28) from three orthogonal perspectives of a  $RHS^2P$  neutrino-e&mvf corresponding to the first great circle magnetic field line and the second great circle electric field line shown with 6 degree increments of the angle  $\theta$ . (Electric field lines red; Magnetic field lines blue).

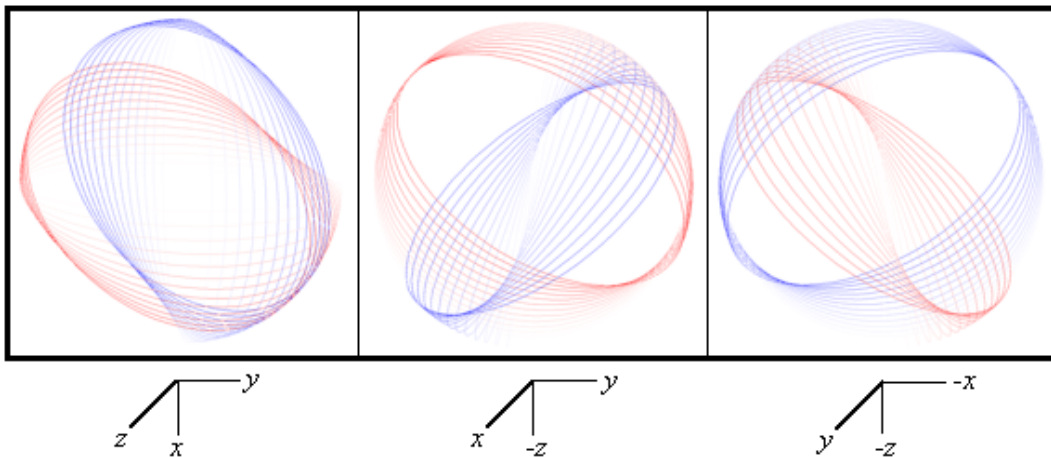


The corresponding antineutrino, the left-hand- $\sin^2 \theta$ -polarized neutrino ( $LHS^2P$ ), is given by is given by:

$$\begin{bmatrix} x' \\ y' \\ z' \end{bmatrix} = \sin^2 \theta \delta(r - r_{\text{photon}}) \begin{bmatrix} \frac{1 + \cos \theta}{2} & -\frac{1 + \cos \theta}{2} & \frac{\sin \theta}{\sqrt{2}} \\ -\frac{1 + \cos \theta}{2} & \frac{1 + \cos \theta}{2} & \frac{\sin \theta}{\sqrt{2}} \\ -\frac{\sin \theta}{\sqrt{2}} & -\frac{\sin \theta}{\sqrt{2}} & \cos \theta \end{bmatrix} \cdot \left( E_0 \begin{bmatrix} 0 \\ r_n \cos \phi \\ r_n \sin \phi \end{bmatrix}_{\text{Red}} + B_0 \begin{bmatrix} r_n \cos \phi \\ 0 \\ r_n \sin \phi \end{bmatrix}_{\text{Blue}} \right) \quad (39.29)$$

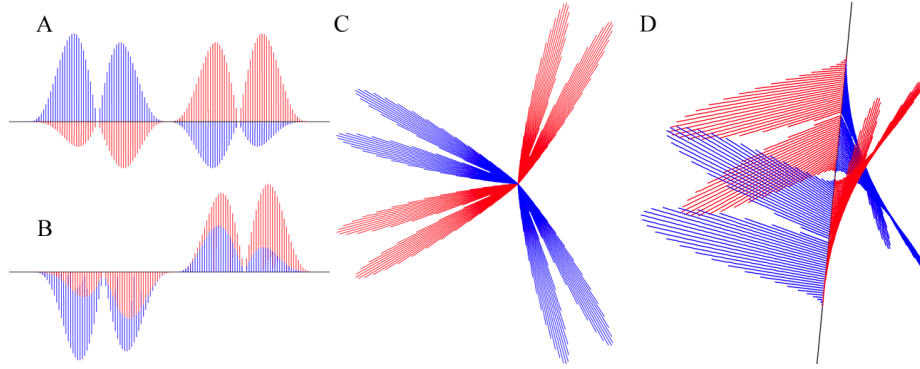
The  $LHS^2P$  neutrino-e&mvf that is generated by the rotation of the great-circle basis elements in the  $xz$ - and  $yz$ -planes about the  $(\mathbf{i}_x, -\mathbf{i}_y, 0\mathbf{i}_z)$ -axis by  $\frac{\pi}{2}$  corresponding to the output of the matrix given by Eq. (39.29) is shown in Figure 39.5.

**Figure 39.5.** The field-line pattern given by Eq. (39.29) from three orthogonal perspectives of a  $LHS^2P$  neutrino-e&mvf corresponding to the first great circle magnetic field line and the second great circle electric field line shown with 6 degree increments of the angle  $\theta$ . (Electric field lines red; Magnetic field lines blue).



The spatial distribution of the field lines of a sine-squared neutrino (Eq. (39.27)) in the inertial frame for the stationary observer or laboratory frame is shown in Figure 39.6.

**Figure 39.6.** The electric (red) and magnetic (blue) field lines of a sine-squared neutrino given by Eq. (39.27) as seen along the axis of propagation in the lab inertial reference frame at a fixed time. A and B. Views transverse to the axis of propagation, the z-axis, wherein  $2r_{\text{neutrino}} = \lambda$ . C and D. Off z-axis views showing field aspects both along and transverse to the axis of propagation.



In this case, Eq. (25) of Appendix V: Analytical-Equation Derivation of the Photon Electric and Magnetic Fields then becomes:

$$\frac{1}{8\pi c} \sqrt{\frac{\epsilon_0}{\mu_0}} \frac{E_0^2}{4} \frac{2\pi}{2\omega} 2\pi r_{\text{photon}}^3 \int_0^\pi \sin^2 2\theta \sin^6 \theta d\theta = \frac{\hbar}{2} \quad (39.30)$$

$$\sqrt{\frac{\epsilon_0}{\mu_0}} \frac{E_0^2}{32c} \frac{2\pi}{\omega} r_{\text{photon}}^3 \int_0^\pi \sin^2 2\theta \left( \frac{1 - \cos 2\theta}{2} \right)^3 d\theta = \frac{\hbar}{2} \quad (39.31)$$

$$\sqrt{\frac{\epsilon_0}{\mu_0}} \frac{E_0^2}{256c} \frac{2\pi}{\omega} r_{\text{photon}}^3 \int_0^\pi \sin^2 2\theta (1 - 3\cos 2\theta + 3\cos^2 2\theta - \cos^3 2\theta) d\theta = \frac{\hbar}{2} \quad (39.32)$$

Using the wave equation relationship and the relationship between the wavelength and the radius of the photon-e&mvf given by Eq. (21) and Eq. (22) of Appendix V, respectively, with the integral by Lide [2] gives

$$\sqrt{\frac{\epsilon_0}{\mu_0}} \frac{E_0^2}{128} \frac{\pi^4}{\omega^4} c^2 \left( \begin{array}{l} \int_0^\pi \sin^2 2\theta d\theta - 3 \int_0^\pi \sin^2 2\theta \cos 2\theta d\theta \\ + 3 \int_0^\pi \sin^2 2\theta \cos^2 2\theta d\theta - \int_0^\pi \sin^2 2\theta \cos^3 2\theta d\theta \end{array} \right) = \frac{\hbar}{2} \quad (39.33)$$

Using the integral #322 and #320 of Lide [2] gives

$$\sqrt{\frac{\epsilon_0}{\mu_0}} \frac{E_0^2}{128} \frac{\pi^4}{\omega^4} c^2 \left( \begin{array}{l} \left( \frac{\theta}{2} - \frac{1}{8} \sin 4\theta \right)_0^\pi - 3 \left( \frac{\sin^3 2\theta}{6} \right)_0^\pi \\ + 3 \left( -64 \sin 8\theta + \frac{\theta}{8} \right)_0^\pi - \left( -\frac{\sin 2\theta \cos^4 2\theta}{10} \right)_0^\pi \\ - \frac{1}{5} \int_0^\pi \cos^3 2\theta d\theta \end{array} \right) = \frac{\hbar}{2} \quad (39.34)$$

$$\sqrt{\frac{\epsilon_0}{\mu_0}} \frac{E_0^2}{128} \frac{\pi^4}{\omega^4 \sqrt{\epsilon_0 \mu_0}} c \left( \frac{\pi}{2} + \frac{3\pi}{8} - \frac{1}{30} \left( \sin 2\theta (\cos^2 2\theta + 2) \right)_0^\pi \right) = \frac{\hbar}{2} \quad (39.35)$$

$$\sqrt{\frac{\epsilon_0}{\mu_0}} \frac{E_0^2}{128} \frac{\pi^4}{\omega^4 \sqrt{\epsilon_0 \mu_0}} c \left( \frac{\pi}{2} + \frac{3\pi}{8} \right) = \frac{\hbar}{2} \quad (39.36)$$

$$\frac{7E_0^2}{1024} \frac{\pi^5}{\omega^4 \mu_0} c = \frac{\hbar}{2} \quad (39.37)$$

Thus,

$$E_0 = \sqrt{\frac{512\omega^4 \mu_0 \hbar}{7c\pi^5}} = \omega^2 \sqrt{\frac{512\mu_0 \hbar}{7c\pi^5}} \tag{39.38}$$

Due to its unusual angular momentum, the antineutrino and neutrino interact extremely weakly with matter. Essentially, it only has a finite cross-section for processes which conserve spin of two fundamental particles participating in a nuclear reaction such as beta decay, inverse beta decay, and photoneutron production reaction (Eq. (5.1191)).



where  $p^+$  is the proton,  $n$  is the neutron,  $\pi^+$  is the positive pion,  $\mu^+$  is the positive muon,  $\nu_e$  is the electron neutrino,  $\nu_\mu$  is the muon neutrino, and  $\bar{\nu}_\mu$  is the muon antineutrino. There are three classes of neutrinos (antineutrinos) corresponding to the electron (antielectron), muon (antimuon), and tau (antitau) as described in the Leptons section. Each flavor corresponds to its multipolarity and polarization,  $\cos^2 \theta$ ,  $\sin^2 \theta$ , and the superposition of  $\cos^2 \theta$  and  $\sin^2 \theta$ . Its particle versus antiparticle type corresponds to its handedness. The determination of the flavor and type assignment can be determined by the multipolarity and polarization and handedness of the particle reaction that gives rise to the neutrino that conserves these aspects as well as energy and linear momentum. The energy of the electric and magnetic fields given by Eq. (1.154) and Eq. (1.263), respectively, equals the energy given by the Planck equation (Eq. (4.8)). The multiplicities and polarizations of photons of visible light change upon interacting with a dichroic material through which they propagate. Similar to dichroism, interconversion of neutrinos may be possible via interaction with matter that causes corresponding changes in multiplicities and polarizations, but due to negligible interaction of neutrinos with matter the interconversion is essentially nil.

Thus, neutrinos are each a type of photon that travels at the speed of light, and each has an exceptional  $\frac{\hbar}{2}$  angular momentum in its electric and magnetic fields giving rise to an intrinsic weak interaction with to nuclei. Light speed is characteristic of and identifies photons, but each has of an angular momentum of  $\hbar$  in its electric and magnetic fields as given in the Equation of the Photon section. Neutrinos have been confirmed to be a type of photon by the measurement of the neutrino velocity with the OPERA detector to be the speed of light to within a relative difference of  $(2.48 \pm 0.28(\text{stat}) \pm 0.30(\text{sys})) \times 10^{-5}$  [3]. Moreover, the speeds of photons and neutrinos are identical within a part per billion from the coincidence of optical and neutrino detection of supernova 1987A [4].

Neutrino interaction with a particle such as absorption requires that the particle possesses current along two orthogonal axes perpendicular to the incident neutrino propagation direction to match the  $\sin 2\theta$  variation of the neutrino E&B fields in space and time. Whereas photon absorption requires that the particle possess current along one axis to match the  $\sin \theta$  variation of the photon E&B fields in space and time as shown in the Equation of the Photon section. The single directional electron current corresponding to spin and orbital angular momentum is given in the One Electron Atom and Excited States of the One Electron Atom (Quantization) sections. Baryons such as protons and neutrons are spin  $\frac{1}{2}$  particles possessing current variation along three orthogonal axes corresponding to current along two orthogonal axes relative to a neutrino propagation direction as shown in the Proton and Neutron section. Furthermore, molecular hydrino such as  $H_2(1/p)$  comprises a paired and an unpaired electron in a single molecular orbital (MO) with a current density function given by  $\frac{1}{2}(\uparrow\uparrow + \downarrow\downarrow)$  wherein the current density function of  $H_2(1/p)$  is given graphically by the sum of current density of Figure 11.2 plus  $\frac{1}{2}$  times the current of Figure 11.2 superimposed on its mirror image as given in the Parameters and Magnetic Energies Due to the Spin Magnetic Moment of  $H_2(1/4)$  section. The net electron spin of  $\frac{1}{2}$  of the  $H_2(1/p)$  MO gives rise to spin flip transitions observed by electron paramagnetic spectroscopy (EPR) and well as magnetism observed by magnetic susceptibility measurements [5-7]. Specifically, Hagen and Mills [6] reported the theoretically predicted g factor for the spin flip transition with the predicted extraordinary features of a series of multiplets due to fluxon linkage within a series of multiplets due to spin-orbital splitting between the diamagnetic paired and paramagnetic unpaired electron of the MO during the EPR transition. The hydrino molecular orbital has current variation along two orthogonal axes and therefore can absorb a neutrino to excite molecular rotation. The rotational energies of low-p-state molecular hydrino correspond to photons in the visible and UV range. The energy of the absorbed neutrino can be admitted as two photons, one from the paired and one from the unpaired electron source currents. Similarly, molecular hydrino can directly absorb and emit two photons or a neutrino during molecular rotational transitions [5]. The space occupied by the hydrino molecular orbital is about 12 orders of magnitude greater than that of a baryon such that the cross-section for neutrino absorption by molecular hydrino is about 12 orders of magnitude higher. The ability to excite neutrino emission using modulatable lasers and neutrino to photon conversion using molecular hydrino detection as part of a heterodyne

detector with a band pass filter is the basis of a telecommunications system that may send essentially unattenuated signals through objects including the Earth. Vulnerable systems such as repeater towers and satellites may be eliminated.

## REFERENCES

1. D. R. Lide, *CRC Handbook of Chemistry and Physics*, 79<sup>th</sup> Edition, CRC Press, Boca Raton, Florida, (1998-9), pp. 11-42.
2. D. R. Lide, *CRC Handbook of Chemistry and Physics*, 79<sup>th</sup> Edition, CRC Press, Boca Raton, Florida, (1998-9), pp. A-38 to A-40.
3. T. Adam, et. al., "Measurement of the neutrino velocity with the OPERA detector in the CNGS beam", Sept., (2011), <http://arxiv.org/abs/1109.4897>.
4. L. M. Krauss, S. Tremaine, "Test of the weak equivalence principle for neutrinos and photons", *Phys. Rev. Lett.*, Vol. 60, (1988), pp. 176-177.
5. R. Mills, "Hydrino States of Hydrogen", [https://brilliantlightpower.com/pdf/Hydrino\\_States\\_of\\_Hydrogen.pdf](https://brilliantlightpower.com/pdf/Hydrino_States_of_Hydrogen.pdf), submitted for publication.
6. Wilfred R. Hagen, Randell L. Mills, "Electron Paramagnetic Resonance Proof for the Existence of Molecular Hydrino", Vol. 47, No. 56, (2022), pp. 23751-23761; <https://www.sciencedirect.com/science/article/pii/S0360319922022406>.
7. Wilfred R. Hagen, Randell L. Mills, "General EPR pattern from molecular hydrino produced in various reactors", (2024), submitted; [https://brilliantlightpower.com/pdf/General\\_EPR\\_pattern\\_from\\_molecular\\_hydrino\\_produced\\_in\\_various\\_reactors.pdf](https://brilliantlightpower.com/pdf/General_EPR_pattern_from_molecular_hydrino_produced_in_various_reactors.pdf).
8. [http://physics.nist.gov/cgi-bin/Compositions/stand\\_alone.pl?ele=H&ascii=html&isotype=some](http://physics.nist.gov/cgi-bin/Compositions/stand_alone.pl?ele=H&ascii=html&isotype=some).
9. J. D. Jackson, *Classical Electrodynamics*, Second Edition, John Wiley & Sons, New York, (1975), pp. 758-763.
10. M. Goldhaber, J. Weneser, *Annual Review of Nuclear Science*, Vol. 5, ed., J. G. Beckerley, Annual Reviews, Stanford (1955), pp. 1-24.
11. T. K. Gaylord, K. F. Brennan, *J. Appl. Phys.*, Vol. 65 (2), (1989), pp. 814-820.
12. A. Beiser, *Concepts of Modern Physics*, Fourth Edition, McGraw-Hill, New York, (1987), pp. 462-467.